IEEE Access
Multidisciplinary | Rapid Review | Open Access Journal

Received December 7, 2019, accepted December 23, 2019, date of publication January 1, 2020, date of current version January 10, 2020.

Digital Object Identifier 10.1109/ACCESS.2019.2963432

A Specific Iterative Closest Point Algorithm for Estimating Radar System Errors

PENGFEI LI[1], EN FAN[2], AND CHANGHONG YUAN[3]
[1]Army Academy of Artillery and Air Defense Forces Zhengzhou Campus, Zhengzhou 450052, China
[2]Department of Computer Science and Engineering, Shaoxing University, Shaoxing 312000, China
[3]Network Center, Southern Medical University, Guangzhou 510515, China

Corresponding author: En Fan (efan@usx.edu.cn)

This work was supported in part by the National Natural Science Foundation of China under Grant 61703280, in part by the Zhejiang Natural Science Foundation under Grant LY20F020011, and in part by the International Science and Technology Corporation Base for Resource and Environment Informationization of Gansu Province.

ABSTRACT A common radar system calibration approach is to use civil aviation automatic dependent surveillance-broadcast (ADS-B) data to register errors. Considering the temporal and spatial uncertainties in radar system observation data, a specific iterative closest point (SICP) algorithm is proposed for estimating two-dimensional (2D) radar system errors. Radar system errors consist of the measurement deviations for the slant range and azimuth of the target and are spatially reflected by the difference between the observed and actual (ADS-B-observed) positions of the same target. Thus, the SICP algorithm is used to register the tracks corresponding to radar and ADS-B observation data. The radar system errors are reflected by a translation, rather than a rotation, of the observation data. Therefore, in the SICP algorithm, a unit matrix first replaces the rotation matrix in the iterative closest point (ICP) algorithm. Then, the translation matrix is iteratively calculated, and finally, the cumulant of the translation matrix is calculated as the radar system error. The proposed algorithm is advantageous because it does not require the temporal registration of radar and ADS-B observation data when temporal and spatial uncertainties are present (e.g., when 2D radar observation data have low accuracy and contain many outliers). Additionally, the SICP algorithm can effectively reduce the dependence on sensor data accuracy. The experimental results obtained based on simulated and measured data demonstrate that compared to conventional registration algorithms, the proposed algorithm can rapidly and accurately estimate radar system errors and has higher registration accuracy.

INDEX TERMS Two-dimensional radar, ADS-B, ICP, system error registration, curve registration.

I. INTRODUCTION

In a radar network system, multiple radars transmit detection data to the data fusion center for data fusion. A precondition for successful multisensor data fusion is that system errors need to be eliminated from the observation data collected by various sensors before the data can be transformed into a common reference coordinate system for processing. If uncompensated, system errors will increase target tracking errors. For a multisensor system, system errors will cause a relatively large difference between the tracks of the same target observed by various radars. This will lead to fuzzy, difficult track association and fusion, which in turn will weaken the radar network system performance in track fusion or even cause it to lose its advantages [1]. System error registration is a key issue that must be addressed in multisensor information fusion. Anti-bias track association algorithms have been proposed for system errors in multisensor information fusion [2]–[5]. By directly substituting the radars' system and random errors into track association algorithms, Qi *et al.* [2] and Qi *et al.* [3] realized track association via two processing steps (coarse and fine). In addition, Qi *et al.* [4] and Dong *et al.* [5] achieved anti-bias track association based on topological relationships. The above track association algorithms can improve association robustness. However, because system errors are not eliminated, these algorithms are unable to improve the sensor tracking accuracy. Hence, to improve fusion quality, it is necessary to first register radar system errors.

Several studies have been conducted to investigate radar system error registration [6]–[15]. Rafati *et al.* [6] registered errors in asynchronous radar observation data collected by

The associate editor coordinating the review of this manuscript and approving it for publication was Guitao Cao.

multiradar network systems. A new real-time radar system error estimation algorithm was also proposed [7]. All of these algorithms use high-accuracy radar data to register other radar system errors. With the continuous development of global navigation satellite systems (GNSSs), the comprehensively use of sensors, (such as GNSSs and radars) in information fusion and error registration has become a new research direction. A method was proposed to comprehensively use radar, global positioning system (GPS), and sonar data to facilitate accurate ship track positioning and tracking through chambers in a lock [8]. This method can effectively improve positioning accuracy. Automatic dependent surveillance-broadcast (ADS-B) technology applied in civil aviation systems uses GNSSs for positioning. Compared to the measuring accuracy of early-warning radars, GNSSs have very high target positioning accuracy. Therefore, the use ADS-B data to achieve real-time registration of radar system errors has great potential. Radar and ADS-B-combined error registration algorithms have been proposed [9]–[11]. However, because ADS-B receivers are unable to obtain accurate data packet transmission times, these algorithms [9]–[11] must estimate new errors that result from time inaccuracies. While these algorithms are able to achieve a relatively high registration accuracy, their engineering applications are, to some extent, limited by their complexity. Based on ADS-B observation data, a combined system error estimation algorithm for radar and ADS-B tracking platforms was proposed [12]–[14]. This algorithm is, however, still relatively highly complex. A multisensor spatial registration algorithm was also proposed based on the entropy function approach [15]. However, this algorithm requires synchronous radar detection, which is difficult to achieve in practical radar networks.

Most of the available radar system error registration algorithms primarily focus on the difference between the radar-observed and actual target positions. These algorithms first require that various information sources have accurate time systems. Because information sources differ in their data update cycles, it is necessary to first use a state-model prediction algorithm to predict point tracks and calculate the difference between observations made at the same time from various information sources. Ultimately, statistical methods are needed to average the errors in all the observation data to estimate radar system errors. However, these approaches still face the following challenges.

(1) When using ADS-B data for error registration, it is impossible to obtain an accurate time for ADS-B data transmission. As a result, it is impossible to temporally align radar and ADS-B observation data, thereby affecting the radar system error estimation accuracy.

(2) To ensure consistency in radar and ADS-B sampling times, it is necessary to correct the sampling times of each sensor by interpolation. Interpolation is an approximate data processing method and thus will introduce new errors into the observation data, reducing the system error estimation accuracy.

(3) Outliers contained in radar observation data will also affect the statistical estimate of radar system errors.

Considering the above problems in system error registration methods, a graphic method may be used to effectively reduce the effects of inconsistent observation data sampling times on system error estimation. From a graphic perspective, a radar bearing system error registration approach was proposed based on multistraight line fusion [18]. In this approach, a nearly straight-line track of the same group of targets is first selected from both the ADS-B and radar track data, the outliers are then removed, the overall least-squares (LS) algorithm is subsequently used to fit each of the ADS-B and radar track observation data to a straight line, and finally, the angle between the two straight lines is calculated and treated as the azimuth component of the system error. Thus, the azimuth component of the radar system error is registered. When using this approach, time alignment does not need to be considered. Straight-line fitting can also effectively reduce the effects of random errors on system error estimation. However, this approach is only able to estimate the azimuth component of the system error; it is unable to estimate the range component of the system error. Based on the above approach [18], the LS algorithm was introduced into radar system error estimation [19]. The LS algorithm can further improve the system error estimation accuracy.

Thus, in this study, based on the graphic approach used in previous studies [18], [19] to register system errors, the specific ICP (SICP) algorithm can be used to register radar system measurement errors. Because this study focused primarily on two-dimensional (2D) radars, pitch (elevation) registration is not considered. However, the proposed SICP algorithm is also applicable to three-dimensional (3D) radars and can be used to register the slant-range, azimuth, and pitch (elevation) components of the system error.

II. RADAR AND THE ADS-B–COMBINED OBSERVATION MODEL

Figure 1 shows a 2D radar and ADS-B–combined observation model. In this model, a 2D radar and an ADS-B device are used to track the same target. The radar system errors are generally estimated based on the observation data for the same cooperative target acquired by the radar and the ADS-B device. To facilitate processing, the observation data obtained by the radar and the ADS-B device are referred to as the radar and ADS-B observations, respectively. In addition, it is assumed that the radar- and ADS-B-observed tracks have been coarsely associated and that they are two types of sensor observation data for the same cooperative target.

Theoretically, the radar observation $\boldsymbol{z}_{R,i}$ is composed of the actual position $\boldsymbol{x}_{R,i}$ of the target, the radar system error $\boldsymbol{b}_R$, and the random error $\boldsymbol{e}_{R,i}$, as follows:

$$\boldsymbol{z}_{R,i} = \boldsymbol{x}_i + \boldsymbol{b}_R + \boldsymbol{e}_{R,i} \tag{1}$$

where $\boldsymbol{z}_{R,i} = [r_{R,i}, \theta_{R,i}]^T$, $\boldsymbol{x}_i = [r_i, \theta_i]^T$, $\boldsymbol{b}_R = [\Delta r_R, \Delta\theta_R]^T$, $\boldsymbol{e}_{R,i} = [v^r_{R,i}, v^\theta_{R,i}]^T$, in which $r_{R,i}$ and $\theta_{R,i}$ are the slant range and azimuth of the radar observation, respectively, r_i and

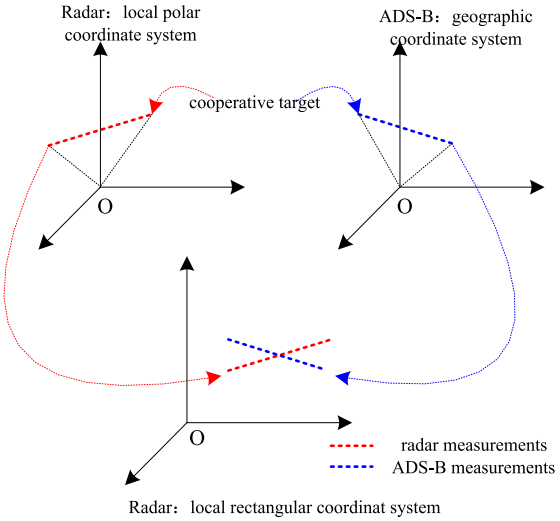

FIGURE 1. Unified observed model for radar and ADS-B device.

θ_i are the slant range and azimuth of the actual position of the target, respectively, and $v_{R,i}^r$ and $v_{R,i}^\theta$ are the slant range and azimuth components of the random error, respectively. In addition, the random error follows a Gaussian distribution, i.e.,

$$\begin{bmatrix} v_{R,i}^r \\ v_{R,i}^\theta \end{bmatrix} \sim \mathrm{N}\left(\begin{bmatrix} 0 \\ 0 \end{bmatrix}, \begin{bmatrix} (\delta_R^r)^2 & 0 \\ 0 & (\delta_R^\theta)^2 \end{bmatrix} \right) \tag{2}$$

where δ_R^r and δ_R^θ are constants.

The ADS-B observation $z_{A,i}$ is derived from the GPS position information by coordinate transformation, and has very high accuracy. Therefore, $z_{A,i}$ can be approximately treated as the actual target position. Thus, Equation (1) can be updated to

$$z_{R,i} = z_{A,i} + b_R + e_{R,i} \tag{3}$$

By identity transformation, we have

$$b_R = z_{R,i} - z_{A,i} - e_{R,i} \tag{4}$$

III. 2D RADAR SYSTEM ERROR REGISTRATION ANALYSIS

It is assumed that the target moves along a straight line at a uniform speed. Figure 2(a) shows the track of the radar observation in a rectangular coordinate system. Figure 2(b) shows the track of the radar observation in a polar coordinate system when the radar has no system or random errors.

In the polar coordinate system, if the radar observation only includes the slant-range component of the system error, then the corresponding track is an upward/downward translation of the actual track. If the radar observation contains only the azimuth component of the system error, the corresponding track is a leftward/rightward translation of the actual track. Therefore, the radar system error denotes the translation of the actual track of the target to the observed track in surveillance space, as shown in Figure 3. In Figure 3, the radar-observed and actual tracks of the target are represented by

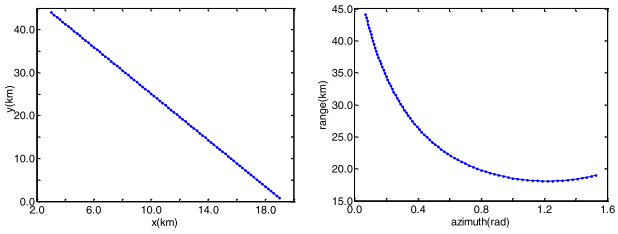

(a) Rectangular coordinative system (b) Polar coordinative system

FIGURE 2. Ideal trajectories of same target in different coordinative systems.

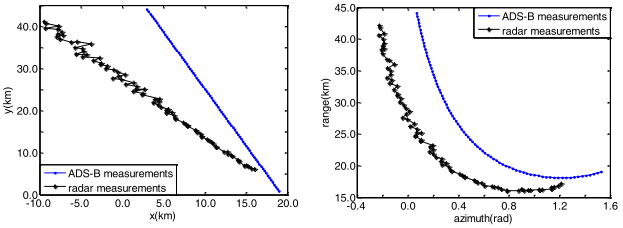

(a) Rectangular coordinative system (b) Polar coordinative system

FIGURE 3. Relationship between real radar and ADS-B measurements.

a dashed star line ("-∗-") and a dash-dotted line ("-.-"), respectively. As shown in Figure 3(b), if the radar observation contains both slant-range and azimuth system error components, then the radar-observed track is a translation of the actual track in each of the two polar coordinate system directions. Therefore, the radar system error can be determined by calculating the extents of translation of the actual track of the target to the radar-observed track.

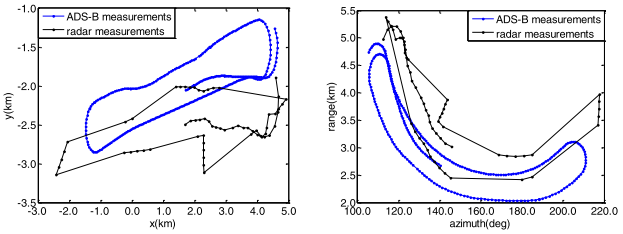

(a) Rectangular coordinative system (b) Polar coordinative system

FIGURE 4. Relationship between real radar and ADS-B measurements.

Figure 4 shows the track of an unmanned aerial vehicle (UAV) monitored by a navigation-monitoring radar. In Figure 4(a), the black track marked by the dashed star line is the flight track of the UAV derived from GPS data, and the blue track marked by the dash-dotted line is the track derived from the navigation radar observation data. As shown in Figure 4(a), there is a significant difference between the radar-observed and ADS-B tracks of the target. As shown in Figure 4(b), the radar-observed track of the target deviates significantly from the ADS-B track in a polar coordinate system.

The above analysis demonstrates that the radar system error consists of the measurement errors for the slant range and azimuth of the target and is spatially represented by

the deviation of the observed position of the target from its true position (i.e., the ADS-B observed position). Therefore, the system error can be determined by registering the to-be-registered curve (the curve corresponding to radar observation) to the standard curve (the curve corresponding to ADS-B data). For accurate registration problems, Besl and McKay [20] innovatively proposed an ICP algorithm. The ICP algorithm is a mainstream algorithm for 3D data registration, and has been extensively applied in accurate registration [21]–[25]. In this study, the ICP algorithm is modified based on the examined application scenario, with the curve corresponding to the radar observation as the point cloud of the target and the curve corresponding to the ADS-B data as the reference point cloud. The SICP algorithm is subsequently used for radar system error estimation.

IV. SYSTEM ERROR REGISTRATION BASED ON THE SICP ALGORITHM

A. OVERVIEW OF THE ICP ALGORITHM

The ICP algorithm is mainly used in 3D model registration. The ICP algorithm registration approach is simple, efficient, accurate, and robust. The basic goal of the ICP algorithm is to find a Euclidean transformation matrix between the target and reference point clouds that ensures an optimal match between the two sets of point clouds under certain measurement standards. The ICP algorithm searches within the reference point set for the point closest to each data point in the target point set during each iteration and treats the two points as a matching point pair. Based on the obtained matching point pairs, the ICP algorithm estimates the transformation parameters. Additionally, the ICP algorithm applies the transformation matrix to the objective function and repeats the iteration process. The ICP algorithm also updates the relative positions of the point clouds. The ICP algorithm repeats this process until the difference between the values of the objective function computed from two consecutive iterations is less than a preset threshold.

Let $\boldsymbol{P} = \{\boldsymbol{p}_i | \boldsymbol{p}_i \in R^2, i = 1, 2, \cdots, N\}$ and $\boldsymbol{Q} = \{\boldsymbol{q}_i | \boldsymbol{q}_i \in R^2, i = 1, 2, \cdots, M\}$ be the target and reference point sets, respectively, where R^2 is a 2D point set and $N \leq M$. The ICP registration algorithm steps are as follows:

(1) Set a threshold $\tau > 0$ as the condition for terminating iterations.

(2) Assume that in the k^{th} iteration, a corresponding $\boldsymbol{q}_i^k$ is found in the reference point set $\boldsymbol{Q}$ for each data point $\boldsymbol{p}_i^k$ in the target point set $\boldsymbol{P}$ that allows $\left\|\boldsymbol{p}_i^k - \boldsymbol{q}_i^k\right\| = \min$

(3) Calculate the rotation matrix $\boldsymbol{R}^k$ and the translation matrix $\boldsymbol{T}^k$ that allows the following:

$$\sum_{i=1}^{N} \left\| \boldsymbol{R}^k \boldsymbol{p}_i^k + \boldsymbol{T}^k - \boldsymbol{Q}_i^k \right\|^2 = \min \tag{5}$$

(4) Calculate $\boldsymbol{p}^{k+1}$ and $\boldsymbol{d}_{k+1}$:

$$\boldsymbol{p}_i^{k+1} = \boldsymbol{R}^k \boldsymbol{p}_i^k + \boldsymbol{T}^k \tag{6}$$

$$d_{k+1} = \frac{1}{N} \sum_{i=1}^{N} ||\boldsymbol{p}_i^{k+1} - \boldsymbol{q}_i^k||^2 \tag{7}$$

If $d_k - d_{k+1} < \tau$, terminate the iteration process; otherwise, return to Step (6) to continue the iteration process.

B. SICP ALGORITHM FOR ESTIMATING THE RADAR SYSTEM ERROR

The radar system error consists mainly of slant-range and azimuth errors. As a result, the curve fitted to the radar observation data is a translation, rather than a rotation, of the curve fitted to the ADS-B observation data. Therefore, the ICP algorithm must be modified for curve registration before it can be used to solve the practical problem investigated in this study. The ICP algorithm can be used to calculate the deviation of the target point set from the reference point set when there is an optimal match between the two curves. There is a curve translation in the application scenario investigated in this study, but no curve rotation occurs. To solve this situation, a unit matrix first replaces the rotation matrix in the ICP algorithm, and we refer to this new algorithm as the SICP algorithm.

The SICP algorithm estimates the radar system error by calculating the deviation between the curves fitted to the radar and the ADS-B observation data in the radar coordinate system. Let us assume that there are M ADS-B observation datasets and N radar observation datasets. Thus, the SICP algorithm registers the error by the following steps:

Step 1: Transform the coordinates of the target's ADS-B observation data

First, the geographic coordinates of the i^{th} ($i = 1, 2, \cdots, M$) target position are transformed to Earth-centered Earth-fixed (ECEF) coordinates (X_i, Y_i, Z_i):

$$\begin{bmatrix} X_j \\ Y_j \\ Z_j \end{bmatrix} = \begin{bmatrix} (N + h_j)\cos\varphi_j \cos\lambda_j \\ (N + h_j)\cos\varphi_j \sin\lambda_j \\ \left[N(1 - \rho^2) + h_j\right]\sin\varphi_j \end{bmatrix} \tag{8}$$

Then, the ECEF coordinates (X_i, Y_i, Z_i) of the target are transformed to to-be-registered radar station-centered local rectangular coordinates. Let (λ_C, ϕ_C, h_C) be the geographic coordinates of the radar station. First, the geographic coordinates (λ_C, ϕ_C, h_C) of the radar station are transformed to ECEF rectangular coordinates (X_C, Y_C, Z_C):

$$\begin{bmatrix} X_C \\ Y_C \\ Z_C \end{bmatrix} = \begin{bmatrix} (N + h_C)\cos\varphi_C \cos\lambda_C \\ (N + h_C)\cos\varphi_C \sin\lambda_C \\ [N(1 - \rho^2) + h_C]\sin\varphi_C \end{bmatrix} \tag{9}$$

Then, (X_i, Y_i, Z_i) are transformed to (x_i, y_i, z_i) using the following equation:

$$\begin{bmatrix} x_i \\ y_i \\ z_i \end{bmatrix} = \begin{bmatrix} -\sin\lambda_C & \cos\lambda_C & 0 \\ -\sin\phi_C \cos\lambda_C & -\sin\phi_C \sin\lambda_C & \cos\phi_C \\ \cos\phi_C \cos\lambda_C & \cos\phi_C \sin\lambda_C & \sin\phi_C \end{bmatrix} \times \left(\begin{bmatrix} X_i \\ Y_i \\ Z_i \end{bmatrix} - \begin{bmatrix} X_C \\ Y_C \\ Z_C \end{bmatrix} \right) \tag{10}$$

Finally, (x_i, y_i, z_i) are transformed to radar-station-centered polar coordinates:

$$\begin{cases} r_i = \sqrt{x_i^2 + y_i^2 + z_i^2} \\ \theta_i = \arctan(x_i / y_i) \end{cases} \tag{11}$$

Step 2: Establish a reference point set and a target point set

The data point set obtained by coordinate transformation of the ADS-B observation data for the target is treated as the reference point set $\boldsymbol{Q} = \{(\theta_i^q, r_i^q)\}$, $j = 1,2,\cdots,M$. The slant range and azimuth data in the radar measurement data are used to form the target point set $\boldsymbol{P} = \left\{\left(\theta_i^p, r_i^p\right)\right\}$, $i = 1, 2, \cdots, N$.

Step 3: Calculate the deviation using the SICP algorithm

The SICP algorithm is applied as follows:

(1) Set a threshold $\tau > 0$ as the condition for terminating iterations.

(2) Assume that in the k^{th} iteration, the reference data point $\boldsymbol{q}_i^k$ closest to each data point $\boldsymbol{p}_i^k$ in the target point set $\boldsymbol{P}$ is found in the reference point set $\boldsymbol{Q}$ that allows $\left\|\boldsymbol{p}_i^k - \boldsymbol{q}_i^k\right\| = \min$.

(3) Calculate the translation matrix $\boldsymbol{T}^k = \left[\Delta\theta^k, \Delta r^k\right]$ that allows

$$\sum_{i=1}^{N} ||\boldsymbol{P}_i^k + \boldsymbol{T}^k - \boldsymbol{Q}_i^k||^2 = \min \tag{12}$$

(4) Calculate $\boldsymbol{p}^{k+1}$:

$$\boldsymbol{p}_i^{k+1} = \boldsymbol{p}_i^k + \boldsymbol{T}^k \tag{13}$$

(5) Calculate the estimation error d_{k+1} between two iterations:

$$d_{k+1} = \frac{1}{N}\sum_{i=1}^{N} ||\boldsymbol{p}_i^{k+1} - \boldsymbol{q}_i^k||^2 \tag{14}$$

If $d_k - d_{k+1} < \tau$, terminate the iteration process; otherwise, return to Step (2) and continue the iteration process.

(6) Terminate the iteration process and calculate the total deviation of the target curve:

$$\beta^{\text{sum}} = \sum_{i=1}^{k} \boldsymbol{T}^i \tag{15}$$

where $\beta^{\text{sum}} = [\Delta\theta^{\text{sum}}, \Delta r^{\text{sum}}]^T$ (Δr^{sum} and $\Delta\theta^{sum}$ are the slant-range and azimuth components of the system error, respectively).

The proposed algorithm can also calibrate low-accuracy radar data against high-accuracy radar data when civil aviation ADS-B devices for cooperative targets are unavailable.

V. EXPERIMENTAL RESULTS AND ANALYSIS

To examine the performance of the proposed SICP algorithm, six system error estimation algorithms, namely, the SICP algorithm, the curve-fitting-based (CF) algorithm, the LS-based algorithm for the radar rectangular coordinate system (LSr), the LS-based algorithm for the radar polar coordinate system (LSp), the curve-fitting-based LS algorithm for the radar rectangular coordinate system (CF-LSr), and the curve-fitting-based LS algorithm for the radar polar coordinate system (CF-LSp), are compared based on measured data.

To facilitate analysis, ADS-B observation data are approximately treated as theoretical values. Additionally, two algorithm evaluation metrics are given.

When the theoretical value of the radar system error is known, the root-mean-square errors (RMSEs) of the radar system error components are used for evaluation, which are defined as follows:

$$\text{RMSE}\left(\Delta\hat{\rho}_R\right) = \sqrt{\frac{1}{M}\sum_{i=1}^{M}\left(\Delta\hat{\rho}_{R,i} - \Delta\rho_{A,i}\right)^2} \tag{16}$$

$$\text{RMSE}(\Delta\hat{\theta}_R) = \sqrt{\frac{1}{M}\sum_{i=1}^{M}(\Delta\hat{\theta}_{R,i} - \Delta\theta_{A,i})^2} \tag{17}$$

where $\Delta\hat{\rho}_{R,i}$ and $\Delta\hat{\theta}_{R,i}$ are the estimated slant-range and azimuth components of the radar system error during the i^{th} experiment, respectively, $\Delta\rho_{A,i}$ and $\Delta\theta_{A,i}$ are the theoretical slant-range and azimuth components of the radar system error during the i^{th} experiment, respectively, and M is the total number of experiments.

When the theoretical radar system error is unknown, the RMSEs of the registered radar observation data are used for evaluation, which are defined as follows:

$$\text{RMSE}\left(\hat{\rho}_R\right) = \sqrt{\frac{1}{N}\sum_{i=1}^{N}\left(\hat{\rho}_{R,i} - \rho_{A,i}\right)^2} \tag{18}$$

$$\text{RMSE}(\hat{\theta}_{R,i}) = \sqrt{\frac{1}{N}\sum_{i=1}^{N}(\hat{\theta}_{R,i} - \theta_{A,i})^2} \tag{19}$$

where $\hat{\rho}_{R,i}$ and $\hat{\theta}_{R,i}$ are the registered slant-range and azimuth components of the radar observation at the i^{th} sampling time, respectively, $\rho_{A,i}$ and $\theta_{A,i}$ are the slant-range and azimuth components of the ADS-B observation at the i^{th} sampling time, respectively, and N is the number of radar or ADS-B observations.

A. EXPERIMENTAL ANALYSIS BASED ON SIMULATION DATA

In the simulation experiments, the following equation was used to model the target motion:

$$3y - 2x - 1600 = 0 \tag{20}$$

where x and y are the horizontal and vertical coordinates of the target on the plane, respectively. The target's initial state was set to $[100\text{m}, 150\text{m/s}, 600\text{m}, 100\text{m/s}]^{\text{T}}$. The blue dash-dotted line in Figure 5(a) shows the target's motion track in the radar rectangular coordinate system. The blue dash-dotted line in Figure 5(b) shows the target's motion track in the radar polar coordinate system. The slant-range and

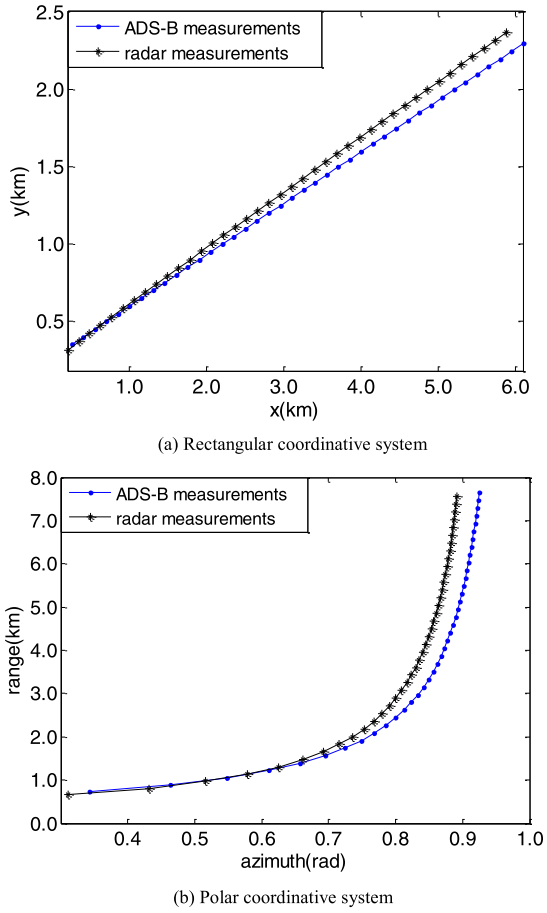

(a) Rectangular coordinative system

(b) Polar coordinative system

FIGURE 5. Radar and ADS-B measurements.

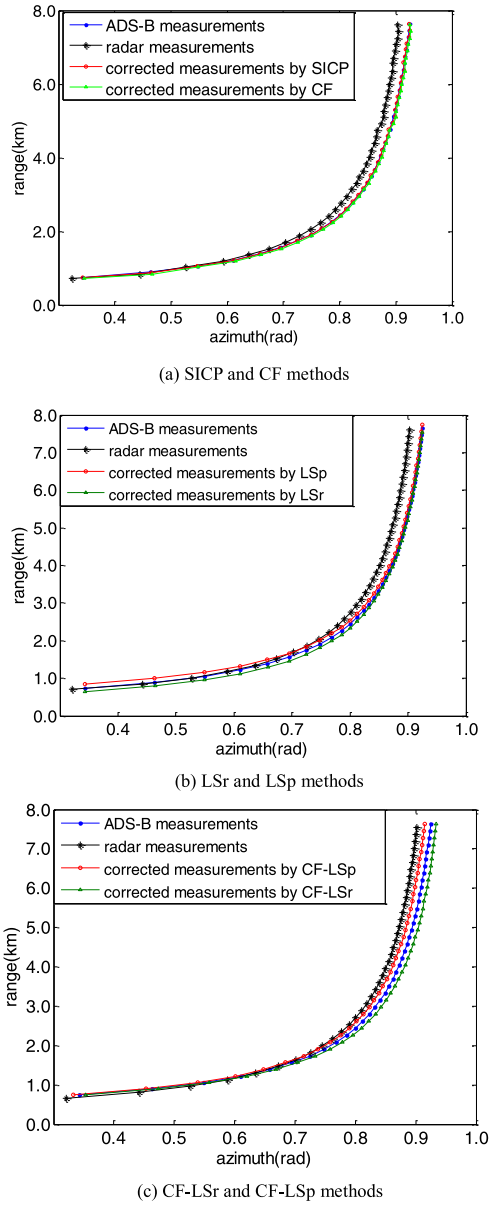

(a) SICP and CF methods

(b) LSr and LSp methods

(c) CF-LSr and CF-LSp methods

FIGURE 6. Registration results of radar measurements in non-delayed situation.

azimuth components of the radar system error were set to $\Delta r_R = 100m$ and $\Delta\theta_R = 0.03$rad, respectively. The random slant-range and azimuth errors were set to $\delta_R^r = 10m$ and $\delta_R^\theta = 0.001rad$, respectively. The sampling period for both the radar and ADS-B device was set to 1 s/time. The black dashed star line in Figure 4 shows the obtained target observation data, including 40 trace points. The ADS-B observations are assumed to contain no system or random errors and are treated as the theoretical target position.

Figure 6 shows the observed tracks of the target registered by the six algorithms in the radar polar coordinate system when the radar sampling times are consistent with the theoretical times. Table 1 summarizes the values of the radar system error estimated by the six algorithms. As demonstrated in Figure 6, the radar observations registered by each of the six system error estimation algorithms are closer to the ADS-B observations, suggesting that all six algorithms are able to improve the accuracy of the radar observation data. For additional clarity, the results obtained using the six algorithms are presented in three plots. Table 1 shows that the values of the radar system error estimated by the SICP and LSp algorithms are the same and are the closest to the theoretical values, suggesting that these two algorithms perform the best in terms of the system error estimation. The system error values estimated by the CF-LSr and CF-LSp algorithms are the second closest to the theoretical values, followed by those estimated by the LSr and CF algorithms. The CF algorithm estimates the azimuth by calculating the angle between the straight lines fitted to the radar and the ADS-B observation data, respectively. Therefore, the CF algorithm is only able to estimate the azimuth component of the radar system error. Additionally, the CF algorithm is also affected by the target motion model. As a result, the CF algorithm performs the worst for system error estimation. However, the CF algorithm is simple and practical. The system error in the CF algorithm-preprocessed radar observation data is relatively small. Consequently, the values of the system error estimated by the LS algorithm in the radar rectangular and polar coordinate

TABLE 1. Estimation results of radar system error.

Methods	Ideal error	**SICP**	CF	LSr	LSp	CF-LSr	CF-LSp
Range (m)	100.00	**96.46**	——	94.79	96.46	96.41	96.46
Azimuth (rad)	0.0300	**0.0284**	0.0332	0.0289	0.0284	0.0381	0.0380

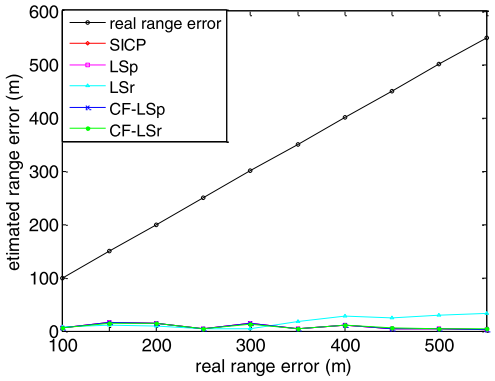

(a) Registration RMSEs in range

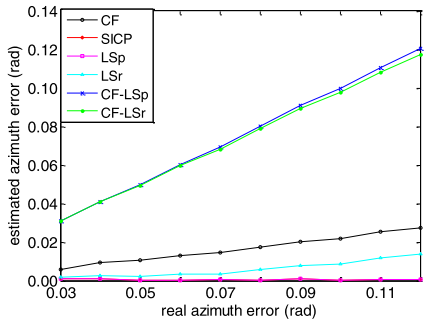

(b) Registration RMSEs in azimuth

FIGURE 7. Registration RMSEs for radar measurements.

systems are basically the same, i.e., the CF-LSr and CF-LSp algorithms have basically the same estimation performance. The system error in the un-preprocessed radar observation data is relatively large. The LSp algorithm outperforms the LSr algorithm, mainly because a nonlinear transformation is required when using the LS algorithm to process radar data in the radar rectangular coordinate system. Additionally, the second- and higher-order system error terms are ignored. This leads to a loss of system error information and thereby affects the system error estimation accuracy. In contrast, in the radar polar coordinate system, the aforementioned processing is not required for the LSp algorithm. Theoretically, after preprocessing the radar observation data, the CF-LSr and CF-LSp algorithms will outperform the LSr and LSp algorithms. However, when the system error is very small, the inversion operation of the matrix in the LS model will be affected, which in turn decreases the estimation accuracy. This is particularly true for estimating the azimuth component of the radar system error.

Figure 7 shows the values of the radar system error estimated by the six algorithms. As shown in Figure 6a, all six algorithms have relatively high estimation accuracy for the slant-range component of the radar system error. In particular, when there is a significant increase in the system error, the estimation accuracy of the six algorithms remains relatively high. Additionally, the six algorithms exhibit relatively similar estimation performance. As demonstrated in Figure 6b, the values of the system error azimuth component estimated by the SICP and LSp algorithms are relatively consistent and have the smallest RMSEs, suggesting that these two algorithms perform the best. The CF-LSr and CF-LSp algorithms exhibit the second best performance, followed by the LSr and CF algorithms. These results are consistent with the experimental results in Table 1.

The estimation performance of the six algorithms is further compared. Table 2 summarizes the mean RMSEs of the aforementioned various components of the system error. As demonstrated in Table 2, the CF-LSp, LSp, and SICP methods exhibit the best performance in estimating the range component of the system error, followed by the CF-LSr and LSr algorithms. The CF-LSr and CF-LSp algorithms have basically the same estimation performance as the LSp and SICP algorithms. The SICP and LSp algorithms exhibit the best performance in estimating the system error azimuth component, followed by the CF-LSp/CF-LSr, LSr, and CF algorithms, in order. Similarly, the CF-LSr and CF-LSp algorithms exhibit basically the same estimation performance. The LSp and SICP algorithms have identical estimation performances.

Figure 8 shows the RMSEs of the data registered by the six algorithms when the radar observation times are inaccurate (there is a time delay in the radar observations; however, the ADS-B observations are still accurately paired with the radar observations). The range and azimuth components of the radar system error are $\Delta r_R = 50m$ and $\Delta\theta_R = 0.02rad$, respectively. The random range and azimuth errors are $\delta_R^r = 10m$ and $\delta_R^\theta = 0.001rad$, respectively. The RMSEs of the registered data are used as evaluation metrics mainly because the system error is unable to completely reflect the estimation algorithm performance when there is a time delay. The RMSEs of the registered data can better reflect the estimation accuracy of the six algorithms. As demonstrated in Figure 8(a), when the time delay is less than 0.8 s, all the algorithms can relatively satisfactorily improve the range component of the radar system error and produce relatively similar estimates, except for the CF algorithm, which is unable to estimate the range component of the system error. A time delay exceeding 0.8 s combined with the flight speed of the target, to some extent, affects the accuracy of the

TABLE 2. Average RMSEs with different radar system errors.

Methods	Average error	**SICP**	CF	LSr	LSp	CF-LSr	CF-LSp
Range (m)	100.00	**12.82**	——	25.19	12.82	12.82	13.18
Azimuth (rad)	0.0300	**0.0011**	0.0173	0.0071	0.0011	0.0346	0.0361

TABLE 3. Registration average RMSEs of radar measurements in delayed situation.

Methods	Ideal error	**SICP**	CF	LSr	LSp	CF-LSr	CF-LSp
Range (m)	——	41.04	50.00	41.41	41.04	41.06	41.04
Azimuth (rad)	——	**0.0001**	0.0031	0.0003	0.0001	0.0010	0.0062

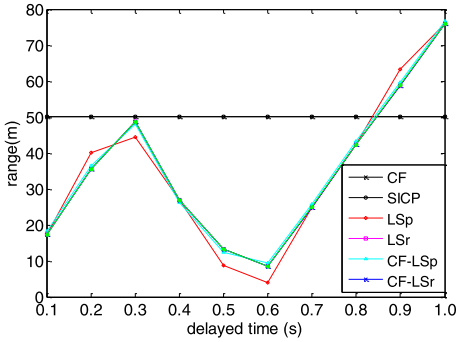

(a) Registration RMSEs in range

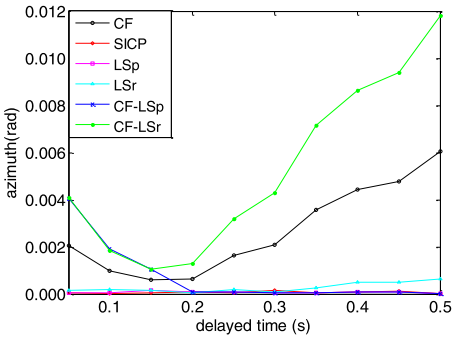

(b) Registration RMSEs in azimuth

FIGURE 8. Registration RMSEs of radar measurements in delayed situation.

radar observation data. The performance of all six estimation algorithms decreases to some extent. Nevertheless, these algorithms are still able to approximately estimate the error in the slant range of the target. Figure 8(b) shows that as the time delay increases significantly, the RMSEs of the data registered by the LSr and CF algorithms also increase significantly, suggesting that these two algorithms are relatively significantly affected by the time delay. In comparison, the other four algorithms are relatively unaffected by the time delay. Table 3 summarizes the mean RMSEs of the data registered by the six algorithms, which more clearly comparatively demonstrate their estimation performance. Table 3 shows that the six algorithms basically exhibit consistent registration performance for the range data. The mean RMSEs of the range data registered by the six algorithms are approximately 41 m. The mean RMSEs of the registered azimuth data show that the CF-LSr algorithm exhibits the best registration performance for the azimuth data, followed by the CF, CF-LSp, LSr, and SICP/LSp algorithms, in order. The SICP and LSp algorithms exhibit the same registration performance for the azimuth data. The results in Table 3 are consistent with those in Figure 8. When there is a system time delay, the registration performance of the CF-LSr and CF algorithms is relatively poor, but the registration performance of the SICP and LSp algorithms remains relatively satisfactory. However, the LSp algorithm requires that the radar observations be accurately paired with the ADS-B observations.

In addition, from Table 1 and Table 3, it is found that the SICP and LSp algorithms obtain the same radar system error and other estimation performance values. This is because the SICP algorithm uses the least squares rule to estimate the bias (the same as the LSp algorithm) between the radar measurements and the ADS-B measurements in the polar coordinate system. Hence, by knowing the observed time of the radar measurements, the SICP and LSp methods can obtain the best performance or approximate the best performance, and they obtain the same values as the experiment results.

In summary, regardless of the accuracy of the radar sampling times (i.e., if there is a time delay), the SICP algorithm is able to produce relatively satisfactory estimates. Additionally, compared to other LS model-based algorithms, the SICP algorithm does require an accurate match between radar and ADS-B observations. Therefore, the simulation experiment sufficiently demonstrates that the SICP algorithm is able to effectively and satisfactorily estimate the radar system error.

B. EXPERIMENTAL ANALYSIS OF MEASURED DATA

To test the effectiveness of the algorithm in this paper, surveillance radar is used to continuously track civil aviation aircraft and obtain the measurement data. At the same time, an ADS-B receiver is used to obtain the observations of the aircraft.

Measured data used in this study originated from radar (30 sampling points) and ADS-B (115 sampling points) observations for the same group of cooperative targets.

TABLE 4. Estimation results of radar measurements.

Methods	Ideal error	**SICP**	**SICPc**	CF	LSr	LSp	CF-LSr	CF-LSp
Range (m)	——	**599.32**	**332.12**	——	417.97	332.12	332.37	332.12
Azimuth (rad)	——	**0.1864**	**0.1690**	0.1708	0.1599	0.1690	0.171	0.173

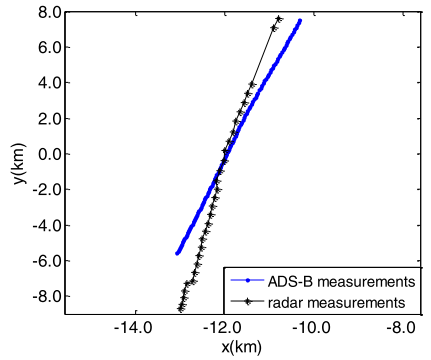

(a) Rectangular coordinative system

(b) Polar coordinative system

FIGURE 9. Radar and ADS-B measurements.

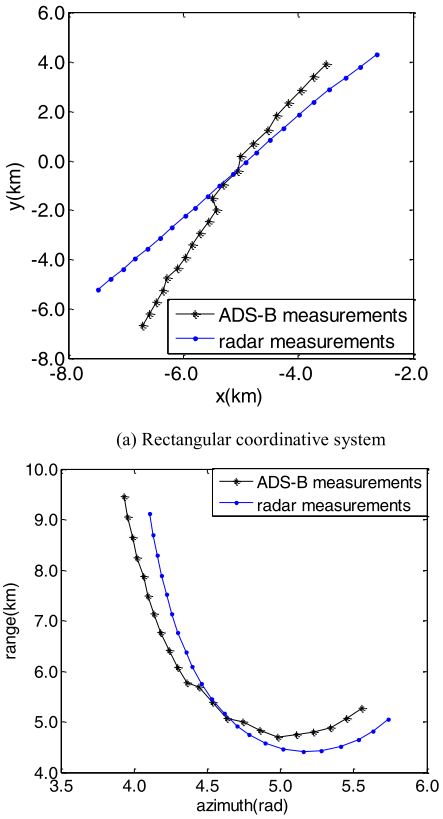

(a) Rectangular coordinative system

(b) Polar coordinative system

FIGURE 10. Radar and ADS-B measurements after preprocessing.

Figures 9(a) and (b) show the trace points of the radar and ADS-B observations at various times in the radar rectangular and polar coordinate systems, respectively. Due to the uncertainties in radar and ADS-B sampling times, it is very difficult to use conventional LS-based radar system error estimation algorithms to establish matching rules for radar and ADS-B observations. In comparison, the SICP algorithm estimates the radar system error by establishing closest matching rules based on the planar geometric constraints for radar and ADS-B observations. As shown in Table 4, the range and azimuth components of the system error estimated by the SICP algorithm are 559.32 m and 0.1864 rad, respectively. Figure 10(a) shows the radar observations registered by the SICP algorithm. As shown in Figure 10(a), the radar observations registered by the SICP algorithm are closer to the ADS-B observations in the radar polar coordinate system. Due to their high accuracy, the ADS-B observations can be approximately treated as the theoretical true target position, which emphasizes the feasibility of the SICP algorithm.

To further analyze the estimation performance of the SICP algorithm, it is assumed that the radar and ADS-B observation sampling times are accurate. The radar and ADS-B observations during a common period of time were selected. Additionally, the ADS-B observations were extrapolated based on the radar sampling times. The extrapolation results are treated as the theoretical values of the radar observations at various times. To facilitate analysis, the radar and ADS-B observations mentioned hereinafter in this section are the selected radar observations during the common period and the extrapolation of the ADS-B observations (each containing 22 sampling trace points), respectively. Figures 10(a) and (b) show the trace points of the radar and ADS-B observations in the radar rectangular and polar coordinate systems, respectively.

Figures 11(b)–(d) show the SICP, CF, LSr, LSp, CF-LSr, and CF-LSp algorithms for the preprocessed radar and ADS-B observations, respectively. Table 4 summarizes the values of the radar system error estimated by these algorithms. To easily distinguish the experiment results of

the SICP algorithm in situations when the sampling time is and is not known, the algorithm is expressed as 'SICPc' when the sampling time is known. The registration results produced by the six algorithms are illustrated in the above three plots, primarily to facilitate demonstration and display. Additionally, to facilitate differentiation, the SICP algorithm for the preprocessed radar data is referred to as the SICP algorithm. As demonstrated in Figures 11(b)–(d), all six algorithms can effectively estimate the radar system error. Based on the difference between the registered radar observations and the ADS-B observations, the SICP algorithm outperforms the CF algorithm, the LSp algorithm outperforms the LSr algorithm, and the CF-LSp and CF-LSr algorithm exhibit similar performances.

Table 5 summarizes the RMSEs of the radar observations registered by the six algorithms and the RMSEs of the radar observations registered by the SICP algorithm for the sampling times and positions. As demonstrated in Table 5, when the sampling times are known, the radar observations registered by the SICPc, CF-LSr, and CF-LSp algorithms have the smallest RMSEs and are the closet to the ADS-B observations (approximately treated as the theoretical position of the target). The RMSEs of the radar observations registered by the CF algorithm are the second smallest, followed by those of the radar observations registered by the LSr and LSp algorithms. This is mainly because the LS algorithms (i.e., the LSp and LSr algorithms) directly process the radar observations, whereas the CF-LS algorithms (i.e., the CF-LSp and CF-LSr algorithms) process the compensated radar observations. Evidently, the error in the radar observation data is significantly greater than that in the compensated radar observation data. In LS estimation modeling, the second- and higher-order terms of the system error are ignored. In fact, these terms also contain system error information and will affect the system error estimation accuracy, particularly when the system error is relatively large, which suggests that LS algorithms are relatively sensitive to observation data errors. Additionally, compared to the LSp algorithm that processes radar observations in the polar coordinate system, the LSr algorithm processes radar observations in the rectangular coordinate system, which requires a nonlinear transformation of the azimuth information. This transformation will cause certain loss of information when the system error is relatively significant. As a result, the estimation accuracy of the LSp algorithm is higher than that of the LSr algorithm. Relatively less information is lost when nonlinearly transforming the azimuth information after compensating the azimuth radar observation data. As a result, the CF-LSp and CF-LSr algorithms exhibit basically the same estimation performance. In addition, when the sampling times are unknown, the SICP results are also listed in Table 5. Although the SICP results in this situation are not as accurate as those when the sampling time is known, the SICP algorithm can still realize the estimation of the radar system error when the sampling time is not known. The other methods cannot estimate the radar system error when the sampling time is not known.

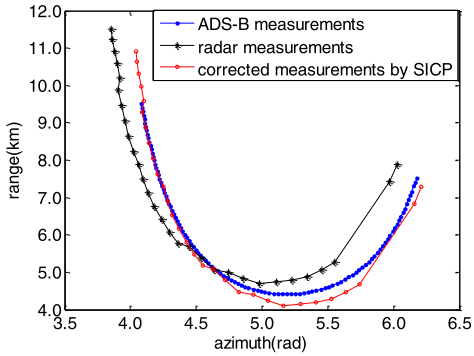

(a) SICP method

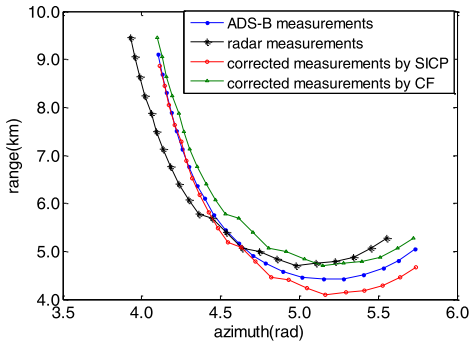

(b) SICP and CF methods

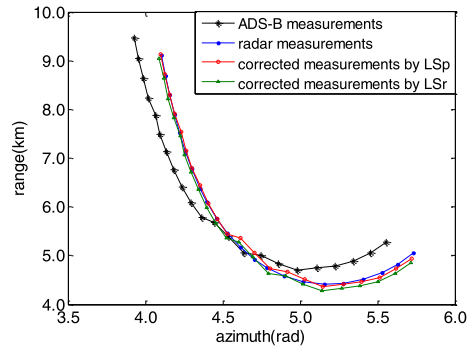

(c) LSr and LSp methods

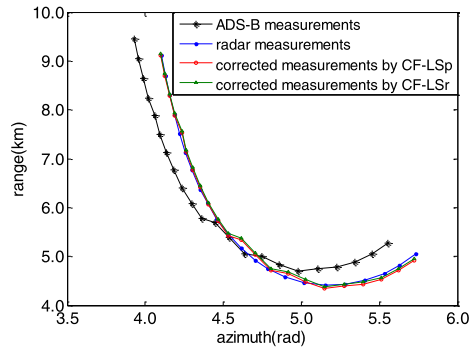

(d) CF-LSr and CF-LSp methods

FIGURE 11. Registration results of radar measurements.

Based on the above analysis, when the radar or ADS-B sampling times are unknown or inaccurate, the SICP algorithm is able to effectively estimate the radar system error

TABLE 5. Registration RMSEs of radar measurements.

Methods	Average RMSEs	**SICP**	**SICPc**	CF	LSr	LSp	CF-LSr	CF-LSp
Range (m)	347.96	**268.44**	**71.03**	374.56	104.92	71.03	71.00	71.03
Azimuth (rad)	0.1687	**0.0203**	**0.0095**	0.0098	0.0128	0.0095	0.0095	0.0095

and improve its observation accuracy. While the CF algorithm is able to more effectively estimate the azimuth component of the radar system error, it is unable to estimate its range component. Additionally, the CF algorithm is only able to effectively perform straight-line fitting and, on this basis, estimate the azimuth component of the radar system error when the target moves in a nearly straight line and the observation data are approximately evenly distributed on the two sides of a straight line, further constricting the application of the CF algorithm. In comparison, the SICP algorithm has a lower requirement for the motion model of the target and a lower time accuracy requirement for radar observations. As a result, the SICP algorithm has a wider range of application. When the radar and ADS-B sampling times are known, the SICP algorithm is also able to produce relatively satisfactory estimates based on preprocessed radar observation data and exhibits the same estimation accuracy as the CF-LSr and CF-LSp algorithms. Therefore, regardless of whether the radar or ADS-B sampling times are known or unknown, the SICP algorithm is able to effectively estimate the radar system error. In particular, when the radar and ADS-B sampling times are known, the SICP algorithm is able to achieve the same estimation performance as the CF-LSp algorithm.

VI. CONCLUSION

In this study, a SICP algorithm is proposed to estimate 2D radar system errors. The SICP algorithm analyzes the radar and ADS-B observation data in the polar coordinate system and considers radar system error estimation from a computer graphics perspective. In other words, when there is a radar system error, the track observed by the radar has the same shape as that observed by an ADS-B device, but there is a deviation between the two tracks. In view of this, the SICP algorithm is established based on the computer graphics approach. The SICP algorithm determines the radar system error by registering the radar-observed curve and calculating the translation matrix between the target and reference curves. This approach cleverly evades the time registration issue. Experiments based on simulations and measured data demonstrate that the SICP algorithm is able to effectively estimate the radar system errors and exhibits excellent radar track registration performance, with promising applications in engineering fields.

ACKNOWLEDGMENT

The authors would like to thank the anonymous reviewers for their valuable comments.

REFERENCES

[1] Y. He, G. H. Wang, and X. Guang, *Information Fusion Theory With Application*. Beijing, China: Publishing House of Electronics Industry, 2010.

[2] L. Qi, K. Dong, Y. Liu, J. Liu, T. Jian, and Y. He, "Anti-bias track-to-track association algorithm based on distance detection," *IET Radar, Sonar Navigat.*, vol. 11, no. 2, pp. 269–276, Feb. 2017.

[3] L. Qi, Y. Liu, and H. L. Ren, "Air-platform multi-radar anti-bias tracks association algorithm," *Acta Aeronautica et Astronautica Sinica*, vol. 39, no. 3, pp. 1–9, Mar. 2018.

[4] L. Qi, Y. He, K. Dong, and J. Liu, "Multi-radar anti-bias track association based on the reference topology feature," *IET Radar, Sonar Navigat.*, vol. 12, no. 3, pp. 366–372, Mar. 2018.

[5] K. Dong, H. P. Wang, and Y. Liu, "Anti-bias track association algorithm based on topology statistical distance," *J. Electron. Inf. Technol.*, vol. 37, no. 1, pp. 50–55, Jan. 2015.

[6] A. Rafati, B. Moshiri, and K. Salahshoor, "Asynchronous sensor bias estimation in multisensory-multitarget system," in *Proc. IEEE Int. Conf. Multi-Sensor Fusion Integr. Intell. Syst.*, 2006, pp. 402–407.

[7] J. B. Portas, J. G. Herrero, and G. De Miguel Vela, "New approach to online optimal estimation of multisensor biases," *IEE Proc., Radar Sonar Navig.*, vol. 151, no. 1, p. 31, 2004.

[8] J. Xiong, L. Shu, Q. Wang, W. Xu, and C. Zhu, "A scheme on indoor tracking of ship dynamic positioning based on distributed multi–sensor data fusion," *IEEE Access*, vol. 5, pp. 379–392, 2017.

[9] H. You, Z. Hongwei, and T. Xiaoming, "Joint systematic error estimation algorithm for radar and automatic dependent surveillance broadcasting," *IET Radar, Sonar Navigat.*, vol. 7, no. 4, pp. 361–370, Apr. 2013.

[10] T. Zhang, X. M. Tang, and L. Jin, "A method of high-accuracy radar calibration with ADS-B," *Acta Aeronautica et Astronautica Sinica*, vol. 36, no. 12, pp. 1–10, Jun. 2015.

[11] W. B. Song, "New algorithm of space registration using cooperative and noncooperative targets," *Telecommun. Eng.*, vol. 53, no. 11, pp. 1422–1427, Nov. 2013.

[12] H. Karniely and H. T. Siegelmann, "Sensor registration using neural networks," *IEEE Trans. Aerosp. Electron. Syst.*, vol. 36, no. 1, pp. 85–101, Jan. 2000.

[13] J. Yan, C. Li, Y. Li, and G. Cao, "Adaptive discrete hypergraph matching," *IEEE Trans. Cybern.*, vol. 48, no. 2, pp. 765–779, Feb. 2018.

[14] W. Cao, Q. Lin, Z. He, and Z. He, "Hybrid representation learning for cross-modal retrieval," *Neurocomputing*, vol. 345, pp. 45–57, Jun. 2019.

[15] J. J. Guo, X. H. Yuan, and C. Z. Han, "A space registration algorithm for multi-sensor target tracking using an entropy function," *J. Xi'an Jiaotong Univ.*, vol. 48, no. 11, pp. 128–134, Nov. 2014.

[16] Y. Zhang, G. H. Wang, and L. Chen, "Real-time robust estimation of sensor bias for radar network under multi-target circumstance," *Electron. Opt. Control*, vol. 20, no. 2, pp. 5–7, Feb. 2013.

[17] J. J. Xiu, G. Y. Wang, and Y. He, "Adaptive tracking and systematic error registration for maneuvering target," *Command Inf. Syst. Technol.*, vol. 9, no. 2, pp. 19–23, Apr. 2018.

[18] P. F. Li, Y. Hao, and H. P. Fei, "Radar calibration error correction algorithm based on segment track linear fitting," *Radar Sci. Technol.*, vol. 15, no. 6, pp. 682–686, Dec. 2017.

[19] C. H. Yuan, W. M. Guo, E. Fan, and P. F. Li, "Least squares radar systematic error estimation algorithm by joint ADS-B," *Comp. Syst. Appl.*, vol. 28, no. 9, pp. 264–270, Sep. 2019.

[20] P. J. Besl and N. D. McKay, "A method for registration of 3D shapes," *IEEE Trans. Pattern Anal. Mach. Intell.*, vol. 14, no. 2, pp. 239–256, Feb. 1992.

[21] B. Peng, *Research on Registration of Point Cloud Data in 3D Laser Scanning*. Tianjin, China: Tianjin Univ., 2011.

[22] Z. B. Lv, *Research and Application of 3D Point Cloud Registration Technology*. Harbin, China: Harbin Engineering Univ., 2011.

[23] R. Wang, W. Zhang, Y. Shi, X. Wang, and W. Cao, "GA-ORB: A new efficient feature extraction algorithm for multispectral images based on geometric algebra," *IEEE Access*, vol. 7, pp. 71235–71244, 2019.
[24] H. Kim, S. Song, and H. Myung, "GP–ICP: Ground plane ICP for mobile robots," *IEEE Access*, vol. 7, pp. 76599–76610, 2019.
[25] H. Liu, T. Liu, Y. Li, M. Xi, T. Li, and Y. Wang, "Point cloud registration based on MCMC–SA ICP algorithm," *IEEE Access*, vol. 7, pp. 73637–73648, 2019.

PENGFEI LI received the B.S. and M.S. degrees from the Air Defense Forces Command Academy, Zhengzhou, China, in 2004 and 2007, respectively, and the Ph.D. degree in signal and information processing from Shenzhen University, Shenzhen, China, in 2010.

He is currently an Associate Professor with the Army Academy of Artillery and Air Defense Forces Zhengzhou Campus, Zhengzhou. His main research interests include multisensory data fusion, multitarget tracking, and nonlinear estimation. He is a member of the Chinese Society of Aeronautics and Astronautics.

EN FAN received the B.S. degree in electronic information science and technology from Hubei Engineering University, in 2006, the M.S. degree in signal and information processing from Nanchang Hangkong University, in 2009, and the Ph.D. degree from Xidian University, China, in 2015. From 2016 to 2019, he held a Postdoctoral position with the ATR Key Laboratory, Shenzhen University, China. He is currently a Lecturer with Shaoxing University. His research interests include multisensor data fusion, multitarget tracking, and uncertain information processing.

CHANGHONG YUAN received the B.S. degree in electronic information engineering from Henan Polytechnic University, Jiaozuo, China, in 2006. He is currently pursuing the M.S. degree in biomedical engineering with Southern Medical University, Guangzhou, China. His main research interests include multisensory data fusion and multitarget tracking.